ACS OMEGA

Article

Cite This: ACS Omega 2018, 3, 7191−7195

Solution-Assembled Ordered Grids Constructed with Silver Nanowires as Transparent Conductive Electrodes

De Li,[†] Tao Han,*[,†] and Haibo Ruan[†,‡]

[†]Chongqing Engineering Research Center for Optoelectronic Materials and Devices, Research Institute for New Material Technology, Chongqing University of Arts and Sciences, No. 319, Honghe Road, Yongchuan District, Chongqing 402160, People's Republic of China

[‡]School of Materials and Energy, University of Electronic Science and Technology of China, No.4, Section 2, North Jianshe Road, Chengdu 610054, China

ABSTRACT: The transparent conductive electrodes (TCEs) composed of silver nanowires (Ag NWs) have shown promising applications recently. In this study, we propose a solution-assembled process to obtain the pattern controllable and uniform-ordered Ag NW grid TCEs by combining with the lithographic technique. The transmittance of Ag NW grid TCEs is controlled by the pattern of grids, but its sheet resistance can be tuned by the diameter of Ag NWs in the grids. As the pattern of grids is fixed, conductive property will improve with the decline of the diameter of Ag NWs. This is a new and efficient strategy to resolve the trade-off between optical transmittance and conductive properties of the random metal nanowire networks for optoelectronic devices.

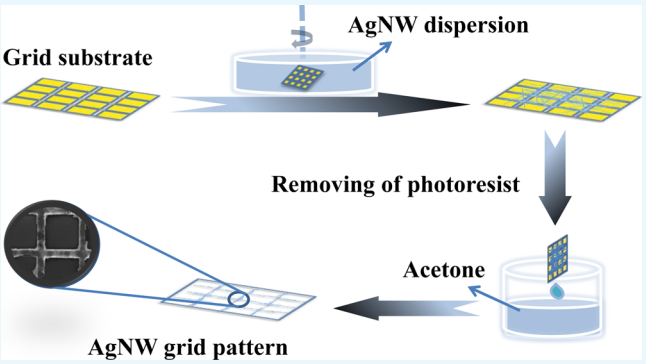

1. INTRODUCTION

In recent years, transparent conductive electrodes (TCEs) have attracted much attention in the fabrication of optoelectronic devices, such as touch-screen displays, organic light-emitting diodes, solar cells, and photodetectors[1,2] Traditionally, indium tin oxide (ITO) electrodes are leading the market of TCEs in optoelectronic devices.[3,4] However, the rarity of indium and the high-cost manufacturing technology have triggered intensive research studies that can simultaneously improve electrical conductivity and optical transmittance.[2,5] So far, to replace ITO, researchers have investigated metal nanowire networks, graphene, carbon nanotubes, percolated metal films, and conductive polymers.[6−11] Of these, metal nanowire-based networks with outstanding physical properties appear to be one of the most promising alternatives to ITO, including Ag, Cu, and Au.[5] Among them, Au NWs are the most expensive and Cu NWs have a great potential to oxidize, which reduces the stability and conductivity of the film.[12−14] Thus, we chose Ag as the raw material for TCEs. At the same time, Ag NWs have a wide range of applications, including flexible transparent conductors, touch panel, electronics, and energy devices.[15−20] However, random metal geometries represent a trade-off between optical transmittance and conductive properties. Thinner and sparser layers provide better optical transmission but reduce the electrical conduction and vice versa.

The metal grid has recently been proven to be a promising structure for high-performance TCEs because of its junction-free characteristic.[21] Unlike random networks, controlled network geometries allow engineered spectral transmission by optimizing trench width. Besides, it is free from moire-pattern problem because of the random nature of the nanowire in grooves.[22] Metal grids can be fabricated by various methods, such as lithographic techniques,[23−27] cracked templates,[28,29] transfer printing,[21] selective laser sintering, and ablation.[30−33] However, many of the nonlithographic approaches or most printing processes typically take a long time to complete because of the serial process. Lithographic methods that fabricated metal-grid-based flexible and stretchable TCEs are more advantageous because of the facile optimization to realize the tunability of optoelectronic performance.

The cost-effective alternatives based on deposition and welding of metal nanowires prepared in solution have proven effective to achieve transparent electrodes with remarkable performances.[5,34−36] The main advantage of a metal nanowire network is the facilitation of a fast path for the nanowire electron conduction through the network.[37] In this work, we demonstrate an approach that combines a lithographic technique and a solution deposition process to fabricate highly controlled two-dimensional networks by using Ag NWs. After embedding Ag NWs in trenches and decomposition of the organic moiety, we obtain pure nanowire grid TCEs. Importantly, the sheet resistance of nanowire grid TCEs can be reduced by decreasing the diameter of Ag NWs. We

Received: June 12, 2018
Accepted: June 21, 2018
Published: July 2, 2018

DOI: 10.1021/acsomega.8b01320
ACS Omega 2018, 3, 7191−7195

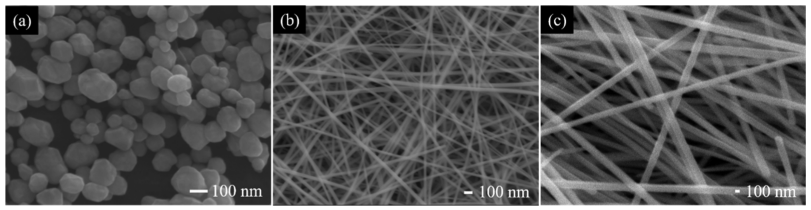

Figure 1. (a) SEM images of Ag nanoparticles, (b) Ag NWs with the diameter of ∼40 nm, and (c) Ag NWs with the diameter of ∼180 nm.

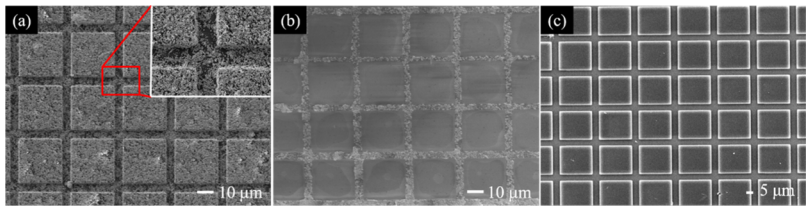

Figure 2. (a,b) SEM images of Ag nanoparticles coated in the grid template and the obtained Ag nanoparticles grid TCEs after photoresist lift-off, respectively. (c) Grid template.

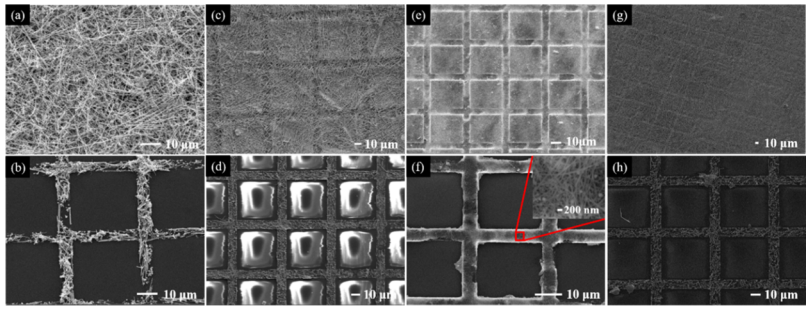

Figure 3. (a), (c), (e), and (g) SEM images of Ag NWs coated in the grid template, S1, and after photoresist lift-off, the obtained Ag NW grid TCEs of (b), (d), (f), and (h) corresponding to (a), (c), (e), and (g). The inset shows the Ag NWs in the grid.

propose an effective strategy to overcome the trade-off between optical transmittance and conductive properties of the random metal nanowire networks.

2. RESULTS AND DISCUSSION

Figure 1a shows the scanning electron microscopy (SEM) images of the Ag nanoparticles and Figure 1b,c shows the SEM images of Ag NWs with an average diameter of ∼40 and ∼180 nm, respectively. The Ag nanoparticles and Ag NWs were synthesized by polyol process. During the synthetic process, with the reduction of $AgNO_3$ and $PtCl_2$ by EG in the presence of polyvinylpyrrolidone (PVP), Ag nanoparticles are first formed via homogeneous nucleation process and heterogeneous nucleation on the platinum seeds. With the addition of Ag^+ continuously, these Ag nanoparticles are monodispersed because PVP macromolecules can chemically absorb onto their surfaces.[38] In addition, some Ag nanoparticles start to dissolve into the solution or grow onto large nanoparticles via a process known as Ostwald ripening.[39] Because of the selective adsorption of PVP molecules, the large Ag nanoparticles are able to grow into rod-shaped structures. Under these conditions, the (100) faces of these rodlike silver structures passivated by PVP molecules and the (111) planes are active for anisotropic growth at [110] direction.

Figure 2a shows the SEM image of Ag nanoparticles coated in the grid template, and the inset image shows partial enlargement. This image demonstrates that the template after filling Ag nanoparticles is uniform. However, the grids are not filled completely. Figure 3b shows the obtained Ag nanoparticle grid TCEs after a photoresist lift-off. The transmittance of Ag nanoparticle TCE is 84%; however, the sheet resistance is 0 because of the intermittent lines of grids. Figure 3c shows the SEM image of the grid template with a wire width of 5 μm and a wire spacing of 25 μm, respectively.

A series of Ag NW grid TCEs were fabricated, and their theoretical transmittance can be calculated according to wire width and spacing, as shown in Table 1. Figure 3 shows that

Table 1. Essential Parameters of Ag NW Grid TCEs

sample	wire width (μm)	wire spacing (μm)	theoretical transmittance (%)	diameter of Ag NWs (nm)
S1	5	25	69.4	∼180
S2	10	50	69.4	∼180
S3	5	25	69.4	∼40
S4	10	50	69.4	∼40

uniformity of the networks over a large area is exhibited in these images. The Ag NWs are spread evenly in the surface of the substrates. After removing the photoresist portion, uniform and clear Ag NW grids are obtained. The interspaces filled with nanowires allow for successful photoresist lift-off because the acetone solution primarily corrodes and removes the photoresist with surface, coated by Ag NWs. The inset in Figure 4f shows tight junction of Ag NWs in the grid.

DOI: 10.1021/acsomega.8b01320
ACS Omega 2018, 3, 7191−7195

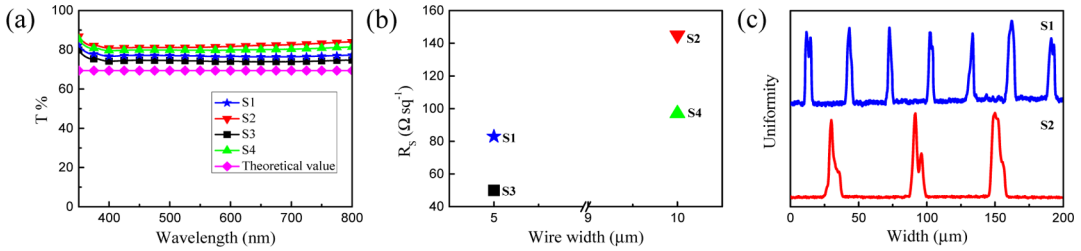

Figure 4. (a) Dependence of transmittance on wavelength. (b) Sheet resistance (dots) values for different wire width of Ag NW grids. (c) Line scans on the surface of samples.

The electrical and optical properties and line scans of the solution-assembled Ag NW grids were characterized in Figure 4. The transmittances of all of the samples are higher than that of the theoretical value, which attributed to the light through the Ag NWs in the grids. By comparing S1 and S2 in Figure 5a,

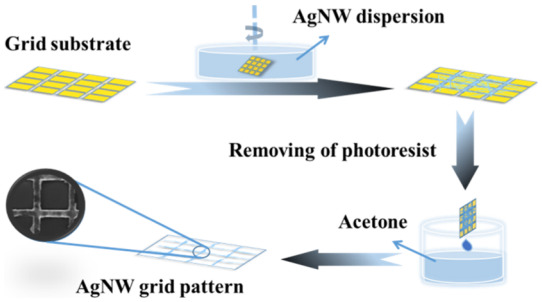

Figure 5. Fabrication process of Ag NW grid TCEs.

when the diameters of the Ag NWs that were filled in S1 and S2 are both 180 nm; the result shows that the transparent electrode with smaller wire width has a lower transmittance which can be attributed to stronger scattering and absorption of light of compact grids.[40] Besides, the conductivity of S1 is better than S2 in Figure 5b. The compact grids fabricated with smaller diameter Ag NWs have better electrical property. When we compare S3 and S4, the result is the same as comparing S1 and S2. When the wire width is same but the diameters of Ag NWs are, respectively, around 180 and 40 nm, S1 with relatively thicker Ag NWs has a better transmittance than that of S3, as shown in Figure 4a. The thinner Ag NWs are stacked closely with each other, leading to a stronger absorption and reflection of incident light, further causing a relatively poor transmission. Besides, the conductivity of S1 is worse than S3 in Figure 5b. These results agree with the fact that the electrode composed of smaller diameter nanowires was reported to have a better conductivity.[41]

Thus, by comparing S1 with S2, the R_s and T increased by 74.7 and 6.0%, respectively. As for S3 and S4, R_s and T are increased, respectively, by 94 and 7.4%. This result shows that the variation of wire width has a greater influence on the R_s relative to T. At the same time, the R_s and T increased, respectively, by 66.0 and 3.3%, by comparing S3 with S1. As for S4 and S2, R_s and T are increased, respectively, by 49.5 and 2.0%. This result shows that the variation of the diameter of Ag NWs has a greater influence on the R_s relative to T. Moreover, R_s is greatly affected by wire width relative to the diameter of Ag NWs through comprehensive comparison. The results show that the transmittance is mainly determined by the pattern of grid, but the sheet resistance can be tuned by the diameter of Ag NWs in the grids. These findings provide an effective strategy to solve the trade-off between optical transmittance and conductive properties of the random metal nanowire networks.

To evaluate the optoelectrical performance of the solution-assembled Ag NW grid TCEs for optoelectronic devices, the figure of merit was theoretically investigated. In general, the figure of merit is defined as the ratio of the electrical conductance (σ_{dc}) and the optical conductance (σ_{Op}), as shown in eq 1

$$T(\lambda) = \left(1 + \frac{188.5}{R_s}\frac{\sigma_{Op}(\lambda)}{\sigma_{dc}}\right)^{-2} \quad (1)$$

where $T(\lambda)$ is the transmission located at 550 nm and R_s is the sheet resistance.[7] The other function for the figure of merit is Φ_{TE}, defined by Haacke,[42]

$$\Phi_{TE} = \frac{T^{10}}{R_s} \quad (2)$$

where T is the transmittance with a pitch at 550 nm. For the high-performance electrode, it is desirable to have a high value of σ_{dc}/σ_{Op} and Φ_{TE}.[36,43,44] The calculated ratio of σ_{dc}/σ_{Op} and Φ_{TE} values are shown in Table 2. As for σ_{dc}/σ_{Op}, the figure of merit is improved with the increase of the grid density and the decline of the diameter of Ag NWs. However, Φ_{TE} is obviously dependent on the diameter of Ag NWs. These results support the strategy to solve the trade-off between optical transmittance and conductive properties. When the Ag NW grid with high transmittance and high grid density is patterned and prepared, we can fabricate the high-performance TCEs with small diameter Ag NWs by the solution process.

Table 2. Summarized T, R_s, Ratio of σ_{dc}/σ_{Op}, and Φ_{TE} Values

sample	T (at 550 nm, %)	R_s (Ω sq^{-1})	σ_{dc}/σ_{Op}	Φ_{TE} (Ω^{-1})
S1	76.7	83	19.9	8.49×10^{-4}
S2	81.3	145	11.7	8.70×10^{-4}
S3	74.2	50	32.5	1.01×10^{-3}
S4	79.7	97	17.3	1.07×10^{-3}

3. CONCLUSIONS

In summary, we combine the substrate lithography and solution process to construct Ag-nanostructured grid TCEs at room temperature, without the need for energy-intensive vacuum metal evaporation processes. This approach also has several other advantages, such as the reusability of Ag nanostructured solution and the compatibility with large area deposition techniques. Besides, this also shows that the

DOI: 10.1021/acsomega.8b01320
ACS Omega 2018, 3, 7191−7195

ordered arrays with solution deposition methods can match the vacuum-based techniques.

The photoelectric performance of the substrate which filled Ag nanoparticles is poor; thus, the sample has not yet met the requirements of the transparent electrode. Furthermore, the transmittance of solution-assembled Ag NW grid TCEs is mainly determined by the structure of the grid, but the sheet resistance can be tuned by the diameter of Ag NWs. Therefore, we present a strategy to handle the trade-off between optical transmittance and conductive properties of the random metal nanowire networks, which is different from the common Ag NW meshes. We can design and prepare the Ag NW grid TCEs with high transmittance and high grid density, by solution assembling the small diameter Ag NWs in the grids. Therefore, this simple strategy can be extended to other types of template-assisted metal nanowire grid TCEs and can provide a general pathway for further optimization of transparent conductor properties at low cost.

4. EXPERIMENTAL SECTION

4.1. Materials. Acetone (99.8%), isopropyl alcohol (99.8%), ethylene glycol (EG, 99.8%), platinum chloride ($PtCl_2$, 99.99%), and $AgNO_3$ (99%) were of analytical grade and purchased from Chengdu Kelong Chemical Corporation. PVP ($M_W \approx 55\,000$, 360 000 and 1 300 000) was purchased from Sigma-Aldrich. All chemicals were used in this work without any further purification. Silver nanowire (average diameter ≈ 40 nm) was purchased from C3NANO INC. All chemicals were used in this work without any further purification.

4.2. Preparation of Ag NWs. All glassware were successively cleaned with deionized water, basic solution, acidic solution, acetone, isopropyl alcohol, and deionized water, respectively. In a typical experiment which synthesizes Ag NWs with an average diameter around 180 nm, 2 mL of 0.1 M $AgNO_3$ EG solution and 2 mL of 0.09 M PVP ($M_W \approx 1\,300\,000$) EG solution were added into a disposable glass, mixed, and stirred evenly. Then, 20 μL of 0.038 M $PtCl_2$ EG solution was injected using a syringe into the mixed solution. Then, the mixed solutions were sealed and incubated at 160 °C for 6 h. Finally, the precipitate was washed with deionized water for five times to remove PVP residue. The products were dispersed into deionized water for further characterization. When mixing PVP ($M_W \approx 360\,000$) with PVP ($M_W \approx 55\,000$) for a weight ratio of 1:1, we got Ag NWs with an average diameter of 40 nm under the same remaining conditions.

4.3. Solution-Assembly of Ag NW Grid TCEs. The fabrication process is illustrated in Figure 5. First, the lithography technology was adopted to make square arrays on a photoresist film which was spin-coated on a glass substrate (wire width 5−10 μm, wire spacing 25−50 μm). Then, the grid glass substrate was cleaned with deionized water and dried in air at room temperature. Second, the grid glass substrate was placed at the bottom of a beaker filled with Ag NW solution (38 mg mL^{-1})and then the beaker was shaken for 1 h. After the process of deposition, the substrate was fully dried in air at room temperature. Third, the substrate was placed at the bottom of a beaker filled with acetone solution and then sonicated at 35 Hz for 2 min to remove the photoresist. Finally, we obtained a substrate with Ag NW grid pattern and then put it in an oven at 120 °C for 5 min.

4.4. Characterizations. The micrographs were observed by SEM (Quanta 250, FEI, USA) with an acceleration voltage of 20 kV. The transmission spectra were acquired by the UV−vis−near-infrared spectrophotometer (UV-2010, G9825A, Agilent Technology, USA) with a blank substrate as the reference. The sheet resistance was obtained via a four-point probe (RTS-5, uncommon, China). The height and width were determined with a profilometer (KLA-Tencor, D-100, California, USA).

AUTHOR INFORMATION

Corresponding Author

*E-mail: danbaiht@126.com (T.H.).

Notes

The authors declare no competing financial interest.

ACKNOWLEDGMENTS

This work was financially supported by the National Natural Science Foundation of China (grant no. 51402032), Chongqing Youth Science and Technology Talent Cultivation Project (grant no. cstc2014kjrc-qnrc40006), Chongqing International Science & Technology Cooperation Program (grant no. cstc2015gjhz0003), and the Chongqing Science and Technology Program (cstc2017jcyjAX0393).

REFERENCES

(1) Ellmer, K. Past achievements and future challenges in the development of optically transparent electrodes. *Nat. Photon.* **2012**, *6*, 809−817.

(2) Hecht, D. S.; Hu, L.; Irvin, G. Emerging transparent electrodes based on thin films of carbon nanotubes, graphene, and metallic nanostructures. *Adv. Mater.* **2011**, *23*, 1482−1513.

(3) Rider, D. A.; Tucker, R. T.; Worfolk, B. J.; Krause, K. M.; Lalany, A.; Brett, M. J.; Buriak, J. M.; Harris, K. D. Indium tin oxide nanopillar electrodes in polymer/fullerene solar cells. *Nanotechnology* **2011**, *22*, 085706.

(4) Tan, Z.; Zhang, W.; Zhang, Z.; Qian, D.; Huang, Y.; Hou, J.; Li, Y. High-performance inverted polymer solar cells with solution-processed titanium chelate as electron-collecting layer on ITO electrode. *Adv. Mater.* **2012**, *24*, 1476−1481.

(5) Ye, S.; Rathmell, A. R.; Chen, Z.; Stewart, I. E.; Wiley, B. J. Metal Nanowire Networks: The next generation of transparent conductors. *Adv. Mater.* **2014**, *26*, 6670−6687.

(6) Kumar, A.; Zhou, C. The race to replace Tin-doped indium oxide: Which material will win? *ACS Nano* **2010**, *4*, 11−14.

(7) van de Groep, J.; Spinelli, P.; Polman, A. Transparent conducting silver nanowire networks. *Nano Lett.* **2012**, *12*, 3138−3144.

(8) Bae, S.; Kim, H.; Lee, Y.; Xu, X.; Park, J.-S.; Zheng, Y.; Balakrishnan, J.; Lei, T.; Kim, H. R.; Song, Y. I.; Kim, Y.-J.; Kim, K. S.; Özyilmaz, B.; Ahn, J.-H.; Hong, B. H.; Iijima, S. Roll-to-roll production of 30-inch graphene films for transparent electrodes. *Nat. Nanotechnol.* **2010**, *5*, 574−578.

(9) Cao, Q.; Hur, S.-H.; Zhu, Z.-T.; Sun, Y. G.; Wang, C.-J.; Meitl, M. A.; Shim, M.; Rogers, J. A. Highly Bendable, Transparent Thin-Film Transistors That Use Carbon-Nanotube-Based Conductors and Semiconductors with Elastomeric Dielectrics. *Adv. Mater.* **2006**, *18*, 304−309.

(10) Tvingstedt, K.; Inganäs, O. Electrode grids for ITO free organic photovoltaic devices. *Adv. Mater.* **2007**, *19*, 2893−2897.

(11) Kim, Y. H.; Sachse, C.; Machala, M. L.; May, C.; Müller-Meskamp, L.; Leo, K. Highly Conductive PEDOT:PSS Electrode with Optimized Solvent and Thermal Post-Treatment for ITO-Free Organic Solar Cells. *Adv. Funct. Mater.* **2011**, *21*, 1076−1081.

(12) Han, S.; Hong, S.; Ham, J.; Yeo, J.; Lee, J.; Kang, B.; Lee, P.; Kwon, J.; Lee, S. S.; Yang, M.-Y.; Ko, S. H. Fast plasmonic laser nanowelding for a Cu-nanowire percolation network for flexible transparent conductors and stretchable electronics. *Adv. Mater.* **2014**, *26*, 5808−5814.

DOI: 10.1021/acsomega.8b01320
ACS Omega 2018, 3, 7191−7195

(13) Han, S.; Hong, S.; Yeo, J.; Kim, D.; Kang, B.; Yang, M.-Y.; Ko, S. H. Nanorecycling: Monolithic integration of copper and copper oxide nanowire network electrode through selective reversible photothermochemical reduction. *Adv. Mater.* **2015**, *27*, 6397−6403.
(14) Stewart, I. E.; Rathmell, A. R.; Yan, L.; Ye, S.; Flowers, P. F.; You, W.; Wiley, B. J. Solution-processed copper-nickel nanowire anodes for organic solar cells. *Nanoscale* **2014**, *6*, 5980−5988.
(15) Lee, P.; Ham, J.; Lee, J.; Hong, S.; Han, S.; Suh, Y. D.; Lee, S. E.; Yeo, J.; Lee, S. S.; Lee, D.; Ko, S. H. Highly stretchable or transparent conductor fabrication by a hierarchical multiscale hybrid nanocomposite. *Adv. Funct. Mater.* **2014**, *24*, 5671−5678.
(16) Cho, J. H.; Kang, D. J.; Jang, N.-S.; Kim, K.-H.; Won, P.; Ko, S. H.; Kim, J.-M. Metal nanowire-coated metal woven mesh for high-performance stretchable transparent electrodes. *ACS Appl. Mater. Interfaces* **2017**, *9*, 40905−40913.
(17) Lee, J.; Lee, P.; Lee, H. B.; Hong, S.; Lee, I.; Yeo, J.; Lee, S. S.; Kim, T.-S.; Lee, D.; Ko, S. H. Room-Temperature Nanosoldering of a Very Long Metal Nanowire Network by Conducting-Polymer-Assisted Joining for a Flexible Touch-Panel Application. *Adv. Funct. Mater.* **2013**, *23*, 4171−4176.
(18) Jung, J.; Lee, H.; Ha, I.; Cho, H.; Kim, K. K.; Kwon, J.; Won, P.; Hong, S.; Ko, S. H. Highly stretchable and transparent electromagnetic interference shielding film based on silver nanowire percolation network for wearable electronics applications. *ACS Appl. Mater. Interfaces* **2017**, *9*, 44609−44616.
(19) Chang, I.; Lee, J.; Lee, Y.; Lee, Y. H.; Ko, S. H.; Cha, S. W. Thermally stable Ag@ZrO 2 core-shell via atomic layer deposition. *Mater. Lett.* **2017**, *188*, 372−374.
(20) Moon, H.; Lee, H.; Kwon, J.; Suh, Y. D.; Kim, D. K.; Ha, I.; Yeo, J.; Hong, S.; Ko, S. H. Ag/Au/Polypyrrole core-shell nanowire network for transparent, stretchable and flexible supercapacitor in wearable energy devices. *Sci. Rep.* **2017**, *7*, 41981.
(21) Kim, H.-J.; Lee, S.-H.; Lee, J.; Lee, E.-S.; Choi, J.-H.; Jung, J.-H.; Jung, J.-Y.; Choi, D.-G. High-Durable AgNi Nanomesh Film for a Transparent Conducting Electrode. *Small* **2014**, *10*, 3767−3774.
(22) Suh, Y. D.; Hong, S.; Lee, J.; Lee, H.; Jung, S.; Kwon, J.; Moon, H.; Won, P.; Shin, J.; Yeo, J.; Ko, S. H. Random nanocrack assisted metal nanowire bundled network fabrication for a highly flexible and transparent conductor. *RSC Adv.* **2016**, *6*, 57434−57440.
(23) Kang, M.-G.; Guo, L. J. Nanoimprinted semitransparent metal electrodes and their application in organic light-emitting diodes. *Adv. Mater.* **2007**, *19*, 1391−1396.
(24) Jang, J.; Im, H.-G.; Jin, J.; Lee, J.; Lee, J.-Y.; Bae, B.-S. A flexible and robust transparent conducting electrode platform using an electroplated silver grid/surface-embedded silver nanowire hybrid structure. *ACS Appl. Mater. Interfaces* **2016**, *8*, 27035−27043.
(25) Kim, D.-J.; Kim, H.-J.; Seo, K.-W.; Kim, K.-H.; Kim, T.-W.; Kim, H.-K. Indium-free, highly transparent, flexible $Cu_2O/Cu/Cu_2O$ mesh electrodes for flexible touch screen panels. *Sci. Rep.* **2015**, *5*, 16838.
(26) Kwak, M. K.; Ok, J. G.; Lee, J. Y.; Guo, L. J. Continuous phase-shift lithography with a roll-type mask and application to transparent conductor fabrication. *Nanotechnology* **2012**, *23*, 344008.
(27) Guo, C. F.; Sun, T.; Liu, Q.; Suo, Z.; Ren, Z. Highly stretchable and transparent nanomesh electrodes made by grain boundary lithography. *Nat. Commun.* **2014**, *5*, 3121.
(28) Han, B.; Pei, K.; Huang, Y.; Zhang, X.; Rong, Q.; Lin, Q.; Guo, Y.; Sun, T.; Guo, C.; Carnahan, D.; Giersig, M.; Wang, Y.; Gao, J.; Ren, Z.; Kempa, K. Uniform self-forming metallic network as a high-performance transparent conductive electrode. *Adv. Mater.* **2014**, *26*, 873−877.
(29) Gupta, R.; Rao, K. D. M.; Srivastava, K.; Kumar, A.; Kiruthika, S.; Kulkarni, G. U. Spray coating of crack templates for the fabrication of transparent conductors and heaters on flat and curved surfaces. *ACS Appl. Mater. Interfaces* **2014**, *6*, 13688−13696.
(30) Suh, Y. D.; Kwon, J.; Lee, J.; Lee, H.; Jeong, S.; Kim, D.; Cho, H.; Yeo, J.; Ko, S. H. Maskless fabrication of highly robust, flexible transparent Cu conductor by random crack network assisted Cu nanoparticle patterning and laser sintering. *Adv. Electron. Mater.* **2016**, *2*, 1600277.
(31) Kwon, J.; Cho, H.; Eom, H.; Lee, H.; Suh, Y. D.; Moon, H.; Shin, J.; Hong, S.; Ko, S. H. Low-temperature oxidation-free selective laser sintering of Cu nanoparticle paste on a polymer substrate for the flexible touch panel applications. *ACS Appl. Mater. Interfaces* **2016**, *8*, 11575−11582.
(32) Hong, S.; Yeo, J.; Kim, G.; Kim, D.; Lee, H.; Kwon, J.; Lee, H.; Lee, P.; Ko, S. H. Nonvacuum, maskless fabrication of a flexible metal grid transparent conductor by low-temperature selective laser sintering of nanoparticle ink. *ACS Nano* **2013**, *7*, 5024−5031.
(33) Hong, S.; Yeo, J.; Lee, J.; Lee, H.; Lee, P.; Lee, S. S.; Ko, S. H. Selective laser direct patterning of silver nanowire percolation network transparent conductor for capacitive touch panel. *J. Nanosci. Nanotechnol.* **2015**, *15*, 2317−2323.
(34) Leem, D.-S.; Edwards, A.; Faist, M.; Nelson, J.; Bradley, D. D. C.; de Mello, J. C. Efficient organic solar cells with solution-processed silver nanowire electrodes. *Adv. Mater.* **2011**, *23*, 4371−4375.
(35) Lee, J.-Y.; Connor, S. T.; Cui, Y.; Peumans, P. Solution-processed metal nanowire mesh transparent electrodes. *Nano Lett.* **2008**, *8*, 689−692.
(36) De, S.; Higgins, T. M.; Lyons, P. E.; Doherty, E. M.; Nirmalraj, P. N.; Blau, W. J.; Boland, J. J.; Coleman, J. N. Silver nanowire networks as flexible, transparent, conducting films: Extremely high DC to optical conductivity ratios. *ACS Nano* **2009**, *3*, 1767−1774.
(37) Lee, P.; Lee, J.; Lee, H.; Yeo, J.; Hong, S.; Nam, K. H.; Lee, D.; Lee, S. S.; Ko, S. H. Highly stretchable and highly conductive metal electrode by very long metal nanowire percolation network. *Adv. Mater.* **2012**, *24*, 3326−3332.
(38) Zhang, Z.; Zhao, B.; Hu, L. PVP Protective mechanism of ultrafine silver powder synthesized by chemical reduction processes. *J. Solid State Chem.* **1996**, *121*, 105−110.
(39) Roosen, A. R.; Carter, W. C. Simulations of microstructural evolution: anisotropic growth and coarsening. *Phys. A* **1998**, *261*, 232−247.
(40) van de Groep, J.; Gupta, D.; Verschuuren, M. A.; Wienk, M. M.; Janssen, R. A. J.; Polman, A. Large-area soft-imprinted nanowire networks as light trapping transparent conductors. *Sci. Rep.* **2015**, *5*, 11414.
(41) Bergin, S. M.; Chen, Y.-H.; Rathmell, A. R.; Charbonneau, P.; Li, Z.-Y.; Wiley, B. J. The effect of nanowire length and diameter on the properties of transparent, conducting nanowire films. *Nanoscale* **2012**, *4*, 1996−2004.
(42) Haacke, G. New figure of merit for transparent conductors. *J. Appl. Phys.* **1976**, *47*, 4086−4089.
(43) Geng, H.-Z.; Lee, D. S.; Kim, K. K.; Han, G. H.; Park, H. K.; Lee, Y. H. Absorption spectroscopy of surfactant-dispersed carbon nanotube film: Modulation of electronic structures. *Chem. Phys. Lett.* **2008**, *455*, 275−278.
(44) Kim, T.; Kim, Y. W.; Lee, H. S.; Kim, H.; Yang, W. S.; Suh, K. S. Uniformly interconnected silver-nanowire networks for transparent film heaters. *Adv. Funct. Mater.* **2013**, *23*, 1250−1255.

DOI: 10.1021/acsomega.8b01320
ACS Omega 2018, 3, 7191−7195